Automated Antibody Characterization and Screening for Array Tomography via Probabilistic Synapse Detection

Anish K. Simhal[1*], Belvin Gong[2], James S. Trimmer[2], Richard J. Weinberg[3], Stephen J. Smith[4], Guillermo Sapiro[1, 5], Kristina D. Micheva[6]

***For correspondence:**
anish.simhal@duke.edu (AKS)

[1]Electrical and Computer Engineering, Duke University, Durham, North Carolina; [2]Department of Neurobiology, Physiology & Behavior, University of California, Davis, Davis, CA; [3]Department of Cell Biology and Physiology, University of North Carolina, Chapel Hill, North Carolina; [4]Synapse Biology, Allen Institute for Brain Sciences, Seattle, Washington, USA; [5]Department of Biomedical Engineering, Department of Computer Science, Department of Mathematics, Duke University, Durham, North Carolina; [6]Molecular and Cellular Physiology, Stanford University School of Medicine, Stanford, California

Abstract

Application-specific validation of antibodies is a critical prerequisite for their successful use. Here we introduce an automated approach for characterization and screening of antibodies against synaptic molecules for high-resolution immunofluorescence array tomography. The method, based on a probabilistic synapse detection algorithm, is designed to provide a robust, flexible, and efficient tool for antibody characterization. By allowing the user to define the molecular composition and size of synapses expected to contain the antigen, the method is applicable to synaptic molecules with different distribution. The output of the algorithm are automatically computed characteristics such as synapse density and target specificity ratio, which reflect the sensitivity and specificity of immunolabeling with a given antibody. These measurements provide an objective way to characterize and compare the performance of different antibodies against the same target, and can be used to objectively select the antibodies best suited for AT, and potentially also for other immunolabeling applications.

Introduction

Antibodies are an indispensable tool for the modern biologist. Their high-affinity binding to specific target molecules makes it possible to detect, isolate, and manipulate the function of these molecules. A staggering number of antibodies are available to the research community, as are many options to make new antibodies. However, since antibodies are biological tools employed in complex systems, they can be very difficult to evaluate and to use in a predictable and reproducible way. Indeed, a large volume of misleading or incorrect data has been published based on results from antibodies that did not perform as assumed (***Anderson and Grant, 2006***; ***Baker, 2015***; ***Rhodes and Trimmer, 2006***).

Recognizing this problem, there has been substantial progress in optimizing antibody production (***Nilsson et al., 2005***; ***Gong et al., 2016***). The importance of establishing reliable practices for antibody use is now widely recognized, and many companies are adopting transparent practices for rigorous antibody validation (***Fritschy et al., 1998***; ***Uhlen et al., 2016***). The performance of antibodies, however, is application-specific (***Lorincz and Nusser, 2008***), and the reliable performance of an antibody in one application does not guarantee its suitability for another application. For example, an antibody that yields a single band on an immunoblot analysis of a tissue homogenate may prove wholly unsatisfactory for immunohistochemistry on sections of fixed tissue. Moreover, the same antibody that yields a robust and specific signal in immunohistochemical labeling of tissue sections prepared under one set of conditions may yield little or no signal on comparable samples prepared under different conditions (***Fritschy et al., 1998***; ***Fukaya and Watanabe, 2000***). For practical reasons, commercial antibodies are routinely tested for a limited number of common applications and sample preparation conditions, leaving it to individual researchers to validate antibodies for other applications and conditions.

The present study addresses the validation of antibodies against synaptic proteins for use in array tomography (AT), a technique which involves immunolabeling and imaging of serial arrays of ultrathin (70 nm) plastic-embedded tissue slices (***Micheva and Smith, 2007***; ***Micheva et al., 2010***). Embedding in resin provides several advantages. The hard plastic matrix allows the tissue to be sectioned into ultrathin slices, greatly improving the resolution possible with light microscopy, as well as permitting visualization of ultrastructure with electron microscopy. The resin matrix also protects the tissue during antibody elution, enabling the acquisition of dozens of immunofluorescence channels via multiple rounds of antibody labeling, imaging and elution. Because the immunoreaction is performed on ultrathin slices, labeling does not suffer from artifacts consequent to the differing permeability of different tissue compartments, which can lead to misinterpretation in analysis of standard pre-embedding immunohistochemistry. However, embedding requires tissue dehydration, infiltration in plastic resin, and subsequent resin polymerization, all of which can modify protein structure and chemical state, with major effects on immunoreactivity. Identifying antibodies that yield robust and specific immunolabeling of target proteins in plastic sections remains a daunting task. Moreover, finding antibodies that selectively label subcellular targets like synapses presents additional challenges, due to the small size, high density, and the overall complexity and diversity of synapses present in mammalian brain samples. In this study, we introduce a new approach to automatically and objectively identify and characterize those antibodies that yield robust and specific immunofluorescent labeling of target molecules localized to specific populations of synapses in plastic-embedded sections from mammalian brain.

An essential criterion for evaluating the performance of an antibody in a given application is whether its labeling pattern is consistent with the known tissue distribution of its target protein. Accordingly, for an antibody against a synaptic protein, the immunolabeling must be localized at synapses; if this requirement is not met, there is no point in further evaluation of the antibody. Though conceptually straightforward, the practical application of this criterion is difficult and often involves a number of subjective and time-consuming decisions. A synapse can be unambiguously identified with electron microscopy, but this method is too time-consuming to be routinely applied for antibody screening. An alternative strategy is to double label the same sample with another antibody already known to localize at synapses, and measure colocalization. This method has been successfully used (***Micheva et al., 2010***; ***Weiler et al., 2014***), but presents a number of difficulties. The immunofluorescent (IF) signal from a synaptic antibody does not provide a simple binary readout of the presence of a synapse, as illustrated by the cartoon in Figure 1. Synaptic proteins are typically at highest concentrations at synapses, but this is not always true, and all proteins are also present to a variable degree at other subcellular locations. Conversely, many synaptic proteins

are found at restricted subsets of synapses, so many synapses may completely lack that protein. In addition to the fluorescent signal from antibodies bound to their target protein, other sources of fluorescence can confuse interpretation, including signal arising from autofluorescent tissue constituents such as lipofuscin granules and blood cells, and signal arising from contamination or from defects such as tissue folds created during sample processing.

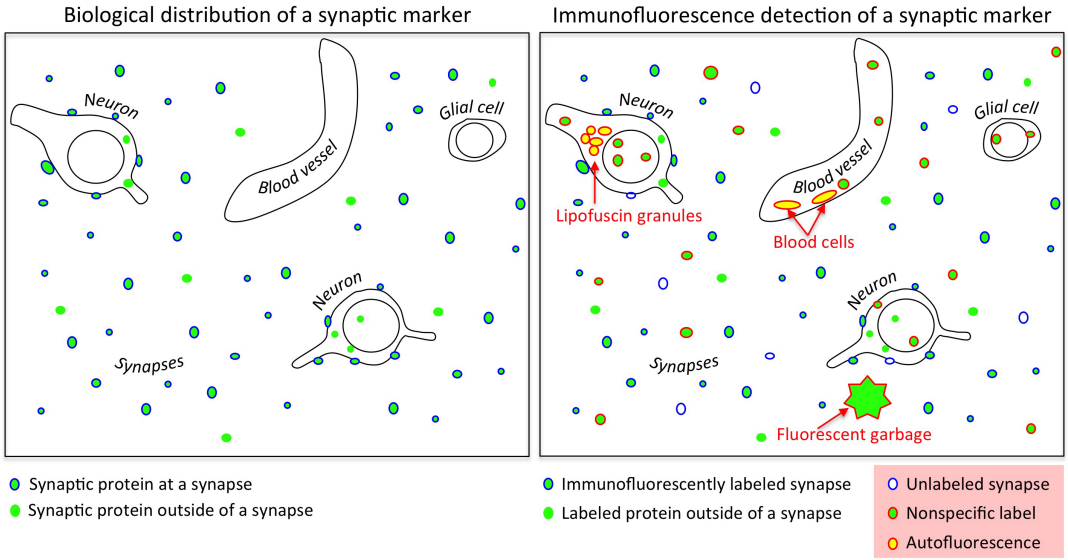

Figure 1. Cartoon of a typical IF image illustrates some of the challenges of antibody evaluation. *A.* Synaptic proteins are found not only at synapses, but also outside of synapses at sites of synthesis and transport; many synaptic proteins also lie in other subcellular compartments reflecting other functions (e.g. as transcription regulators). *B.* Immunofluorescence detection of synaptic proteins is confounded by nonspecific binding of antibodies, low efficiency of target protein detection, fluorescent contaminants, and tissue autofluorescence (e.g. lipofuscin granules, or blood cells).

An efficient and robust method for evaluation of synaptic antibodies should therefore be able to detect individual synapses with high reliability, should provide quantitative measurements of both the intensity and specificity of the immunolabel, and should be rapid and automated. Among the existing computationally-based synapse detection methods for AT (***Busse and Smith, 2013***; ***Collman et al., 2015***), the probabilistic synapse detector, introduced in ***Simhal et al.*** (***2017***), meets all these requirements as a critical building block for antibody characterization. The key feature of the probabilistic synapse detector is that it is query-based, meaning that the user defines the expected molecular composition and size. This flexibility is advantageous for synaptic antibody characterization and screening because the query can be designed to detect different synapse subtypes, depending on prior biological knowledge (e.g., where the antibody target is expected to be located) and depending on the particular goal of the tested antibody. The algorithm can be used for new datasets without creating extensive manual annotations for each synapse subtype, unlike traditional classifiers such as support vector machines and deep learning, used by other synapse detection algorithms (***Bass et al., 2017***; ***Busse and Smith, 2013***; ***Collman et al., 2015***; ***Fantuzzo et al., 2017***; ***Kreshuk et al., 2014***). The results of the detector allow the user to choose different antibody characterization criteria (formally defined below) such as 'synapse density' or 'target specificity ratio' to evaluate the sensitivity and specificity of immunolabeling with a given antibody. The flexibility of this approach makes it a powerful tool for automated evaluation and quantitative comparison of multiple synaptic antibodies for AT, and potentially also for other immunolabeling applications, especially those using immunolabeling of plastic-embedded sections.

Results

The Probabilistic Synapse Detector as an Antibody Characterization Tool

Our approach to characterizing antibodies for AT immunolabeling of brain sections involves computing a series of quantitative characteristics by exploiting and extending a probabilistic query-based synapse detector (***Simhal et al., 2017***). The selected computed characteristics (often denoted as 'measurements' in this manuscript) provide unbiased quantitative information to help evaluate the specificity and sensitivity of immunolabeling obtained with a given antibody. The approach is outlined in Figure 2.

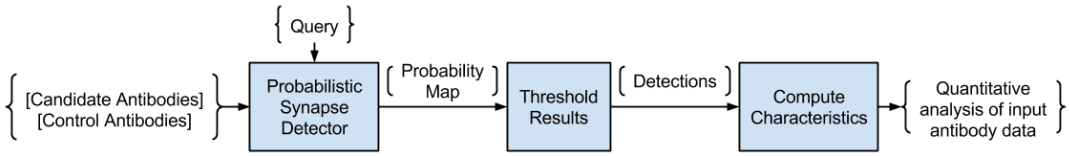

Figure 2. Pipeline of the proposed automated antibody characterization method. The automatic probabilistic synapse detector, using queries designed to study desired properties of the antibody, analyzes the image with the antibody under consideration (see also Figure 4). Then basic characteristics (measurements) of the detected synapses are computed, and these are used for a quantitative analysis of the antibody's effectiveness.

The proposed method is currently optimized for AT immunofluorescence data. Each dataset is composed of multichannel stacks of images from serial sections with (for the current data acquisition protocol) 100 x 100 nm pixel size and 70 nm slice thickness. In each dataset, candidate antibodies against a target protein of interest are tested alongside previously-validated reference antibodies. The synapse detection algorithm is used to automatically detect the probable presence of synapses and quantify the candidate antibody label in relation to these putative synapses. Generally, at least two known synaptic markers are required to detect a synapse. Therefore, some of the datasets contain two control antibodies to facilitate synapse detection, in addition to the candidate antibody (Figure 3). However, when screening multiple candidate antibodies, it is important to minimize the time and cost of the screen. When performed with caution using appropriate antibody combinations, even a single pre-validated antibody can generate interpretable synapse-specific data, and therefore many datasets contain only one control antibody. For example, Figures 3A and 3C provide schematic diagrams of the data used to test a new gephyrin antibody. Gephyrin is known to be highly enriched at the postsynaptic sites of inhibitory synapses (***Sheng and Kim, 2011***). In this case, it is evaluated together with immunolabeling for glutamate decarboxylase (GAD), a protein specific to presynaptic terminals of GABAergic inhibitory synapses for which well-validated antibodies have already been identified. In AT immunofluorescence image data, immunolabeling for synaptic proteins appears as small blobs (typically $< 1\ \mu$m diameter), which will be referred to as 'puncta.' Because synaptic structures are larger than the thickness of individual sections (70 nm), the blobs corresponding to proteins that are abundant throughout the presynaptic or postsynaptic side span several sections and thus form 3D puncta. Our experiments confirm that such minimal use of control antibodies is sufficient to identify the most promising antibodies against a specific synaptic target protein.

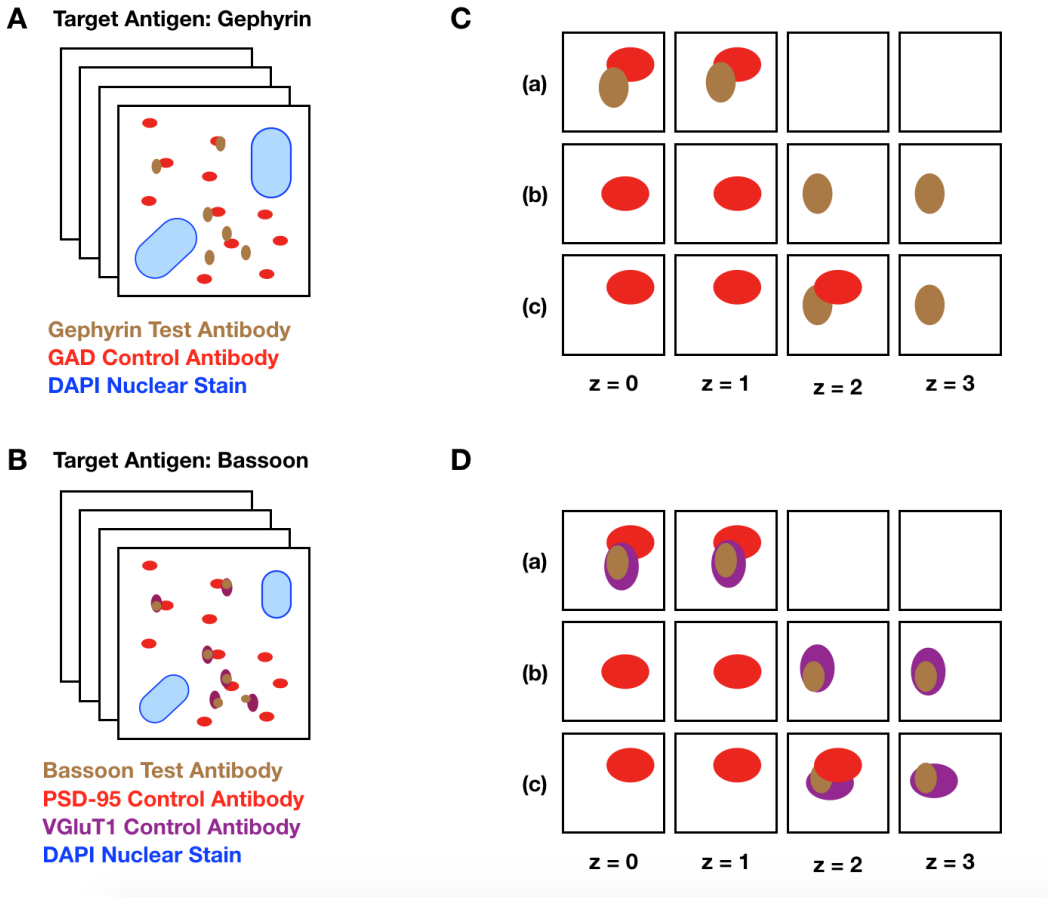

Figure 3. Schematic diagram of an input dataset. *A.* The target protein, gephyrin, is a postsynaptic protein at inhibitory synapses, expected to be adjacent to GAD, an abundant presynaptic protein at inhibitory synapses. The set of squares represents a stack of images from serial ultrathin sections from mouse cortex, double labeled with a gephyrin candidate antibody and a previously validated antibody against GAD. The probabilistic synapse detector algorithm detects the association of gephyrin immunolabel (brown dots) with GAD immunolabel (red dots). The large blue blobs represent DAPI, a marker for cell nuclei. *B.* Identical setup as *A* with bassoon as the target protein. In this example, the tissue is labeled with two control antibodies, VGluT1 and PSD-95. *C.* Different combinations of puncta that can be detected on slices through a synapse. Each row is an example of a possible combination of puncta detected with a query setting the minimum number of slices spanned by each marker to two. Each column shows data from a single thin section of tissue. The red and brown ovals represent presynaptic and postsynaptic markers. In row (a), the two markers lie adjacent on the same z slice. In row (b), the markers lie adjacent in the z direction (across multiple slices). In row (c), the markers colocalize both in the same plane and across multiple slices. Since the probabilistic synapse detector algorithm works in 3D space, it is able to detect synapses where corresponding presynaptic/postsynaptic markers do not lie in the same z plane. *D*. Identical setup as *C* with two control antibodies depicted.

In addition to the image data, the input to the method is a query, which defines the synapse subtype and synapse size (Figure 4). Synapse subtype determines the protein composition of the synapse of interest. For example, if the target protein for which an antibody is being evaluated is localized at inhibitory synapses (as is the case with gephyrin) and the tissue is labeled with an antibody against GAD, then the corresponding query would be to look for synapses containing immunolabeling for gephyrin and GAD, as highlighted by Panel B of Figure 3. If the target protein of interest is instead localized to excitatory synapses, the query may include proteins specific to excitatory synapses such as the postsynaptic protein PSD-95 (postsynaptic density 95) or the presynaptic protein VGluT1 (vesicular glutamate transporter 1).

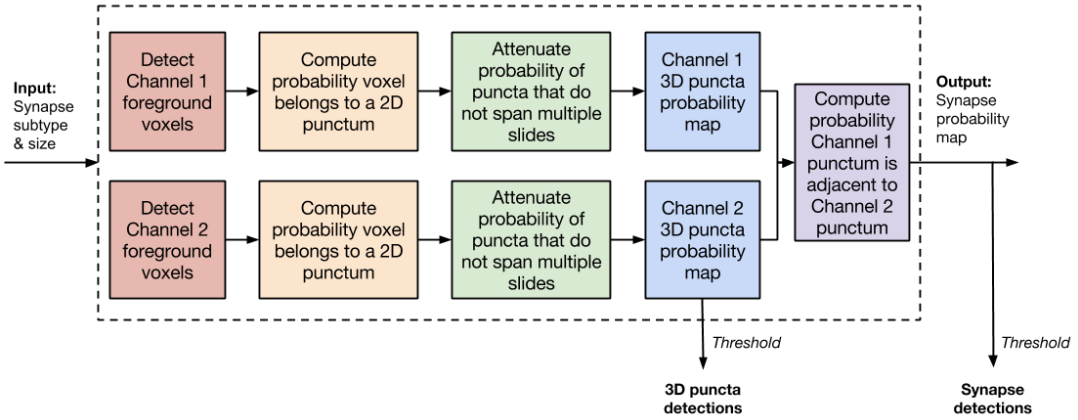

Figure 4. Flowchart of the probabilistic synapse detector used to evaluate synaptic markers for IF AT. This provides the building block for antibody characterization by automatically detecting synapses and their core components, expected to be labeled by the tested antibodies.

The second part of the query is the expected synapse size. Requiring a minimum 3D size minimizes the impact of random specks of noise generated during the image acquisition process and ensures that the immunolabeling is appropriately expressed across slices. For instance, a target protein that is abundantly expressed at a synapse, such as synapsin, should be detected across multiple slices at the current working resolution. Therefore, the presence of a punctum in only one slice likely indicates random noise, nonspecific labeling or fluorescent contaminant. On the other hand, there is little reason to assume that less abundant target proteins or those present at isolated nanodomains within synapses (e.g., many receptors or ion channels) need to span multiple slices through a synapse. The flexible nature of the query allows for the search of synapses of different sizes. A query consisting of GAD and gephyrin puncta spanning three or more slices will return only large synapses, whereas a query consisting of GAD and gephyrin puncta spanning only a single slice would include much smaller synapses. This intrinsic adaptability of the query-based system is critical for automated antibody characterization, allowing the user the flexibility to ask appropriate questions.

Once a query is determined, the probabilistic synapse detector goes through a sequence of steps, first separately analyzing the individual channels composing the query to detect puncta, and then using the morphological relationship between the puncta in the different channels to detect synapses. The output from each individual channel is a 3D volume whose value at each voxel is the probability it belongs to a 3D punctum. The final output of the probabilistic synapse detector is a 3D volume whose value at each voxel is the probability that it belongs to a synapse, as defined by the query (Figure 4). To obtain the putative 3D puncta and synapse detections, these outputs may be thresholded if desired. The threshold level can be determined in a variety of ways (see ***Simhal et al.*** (***2017***) for a detailed discussion). For the experiments in our antibody characterization framework, the threshold was set to a probability value of 0.9 across all datasets. After thresholding, the binarized 3D puncta and synapse detections are used to compute a series of characteristics (measurements, see Methods), including punctum density, punctum volume, synapse density and (computational) target specificity ratio (the fraction of all computationally detected puncta that are associated with synapses), to quantify the data.

This proposed computational antibody characterization method was tested in three different tasks:

1. Pairwise comparisons: Comparing the performance of two different antibodies directed

against the same synaptic target protein.

2. Concentration comparisons: Comparing the performance of the same antibody at different concentrations.
3. Evaluating candidate monoclonal antibodies: Ranking the performance of multiple candidates from monoclonal antibody projects.

The first and second task are conceptually straightforward and involve only antibodies that are already known to recognize the protein in plastic sections, but the third task is much more complicated, because it involves the evaluation of multiple antibody candidates whose suitability for AT has not yet been determined, and whose concentration is not known. The tissue used for this project was from mouse neocortex and was prepared and imaged using standard AT methodology (***Collman et al., 2015***; ***Micheva et al., 2010***).

Pairwise Comparisons

When two well-performing antibodies are available for use in a specific application, which one is better? This is a common question faced by researchers using immunolabeling. Because this question has only three possible answers (one antibody, the other, or they are equal), this was the first task used to validate the proposed method. In each case, the two antibodies were already known to bind their target protein in AT applications, and were used at concentrations previously determined to yield optimal immunolabeling. These antibody pairs were evaluated alongside an antibody for a different synaptic target protein, thoroughly validated for AT in prior studies (***Micheva et al., 2010***; ***Weiler et al., 2014***). Examples of the immunolabeling for each pairwise comparison are shown in Figure 5. Each dataset was independently evaluated and ranked by an expert observer (KM) based on visual examination of the immunolabeling, for which the higher scoring antibody was judged to be the one that had more puncta associated with the control antibody (i.e., labels more synapses, true positives) and/or fewer puncta not associated with the control antibody (false positives). For example, PSD95R had more puncta adjacent to synapsin, without noticeably more synapsin-unrelated puncta, and was therefore evaluated as better performing than PSD95M. Cav3.1R had more puncta that are not adjacent to VGluT1, and also displayed nonspecific labeling of the cell nucleus, and was therefore judged to perform worse than Cav3.1M. In the VGluT1 example, the difference between the two antibodies was subtle, as shown by the measurements of synaptic density and target specificity (see Table 1).

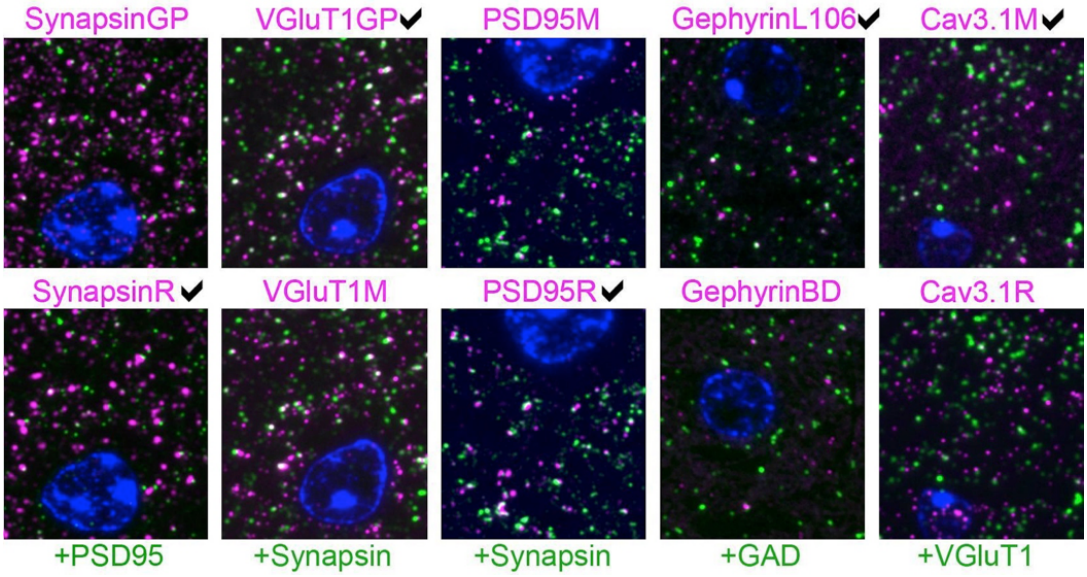

Figure 5. Pairwise comparison of immunofluorescence on single sections from mouse brain. Each column represents an experiment where two antibodies against the same target protein (magenta) are evaluated by double labeling with a control antibody (green). The expert's preference is marked for each column. The sections are also labeled with the nuclear stain DAPI (blue). For each experiment, the two images are from the same section, except for the gephyrin results, where immunolabeling with the two gephyrin antibodies was performed on different sections. Close proximity (when the antibodies are against a presynaptic and a postsynaptic protein: all but one case) or overlap (when the immunolabels are for the same synaptic compartment: VGluT1 experiment) of the magenta and green channels suggest the presence of a synapse. Each image is 16x18 μm.

Target Protein	Tested antibodies	Control Antibody	Punctum density / μm^3	Average punctum size / standard deviation (pixels)	Synapse Density / μm^3	Target Specificity Ratio
Synapsin	Synapsin GP	PSD-95	2.01	15.9 / 59.4	0.55	0.27
	Synapsin R		1.09	27.0 / 48.6	0.49	0.45
VGluT1	**VGluT1GP**	Synapsin	1.54	12.1 / 30.2	0.43	0.28
	VGluT1M		1.27	11.0 / 22.3	0.32	0.25
PSD-95	PSD-95m	Synapsin	0.95	10.7 / 101.7	0.53	0.56
	PSD-95r		1.14	25.4 / 39.9	0.79	0.69
Gephyrin	**GephyrinL106**	GAD	0.72	12.5 / 94.1	0.13	0.18
	GephyrinBD		0.46	17.9 / 263.1	0.08	0.17
Cav 3.1	**Cav3.1M**	VGluT1	0.58	7.4 / 14.0	0.33	0.56
	Cav3.1R		1.22	8.6 / 52.23	0.33	0.27

Table 1. Results from pairwise antibody comparisons. Punctum density, average punctum size, and standard deviation of punctum size were all computed for the tested antibody in question. The names in bold in the second column represent the antibodies preferred by an expert based on visual examination. In each case, the automated synapse detection system would select the same antibody as the expert observer.

These antibody pairs were independently evaluated using the probabilistic synapse detector. For each dataset, the minimum expected marker size (query) was set at 0.2x0.2x0.14 μm, corresponding to 2 pixels by 2 pixels by 2 slices. For each of these pairwise comparisons, two measures, synapse

density and target specificity ratio, were used to rank the two candidate antibodies (Table 1). When the antibodies are used at their optimal concentration, a higher measured synapse density implies higher sensitivity of the antibody (since it detects the target protein at more synapses). A higher target specificity ratio (i.e., a higher proportion of detected immunolabeled puncta that are associated with synapses) indicates higher selectivity of the antibody for the protein of interest. In each of the five cases, the antibody that scored higher with the automated synapse detection algorithm was the same one that was visually identified by the expert as yielding the more robust and specific pattern of immunolabeling. VGluT1 and PSD-95 antibodies scored higher on both sensitivity (synapse density) and specificity (target specificity ratio), while others scored higher on only one of these measures. In the cases of Cav3.1 and synapsin, the higher-scoring antibodies had higher target specificity ratio but gave synaptic densities comparable to the other antibody. In the case of gephyrin, both antibodies had similar target specificity ratio, but the higher-ranked antibody had a higher synaptic density. These results illustrate the importance of using complementary measurements for antibody evaluation. Conveniently, the proposed framework provides multiple objective computations, and the user can pick the most suitable one(s) for a given task.

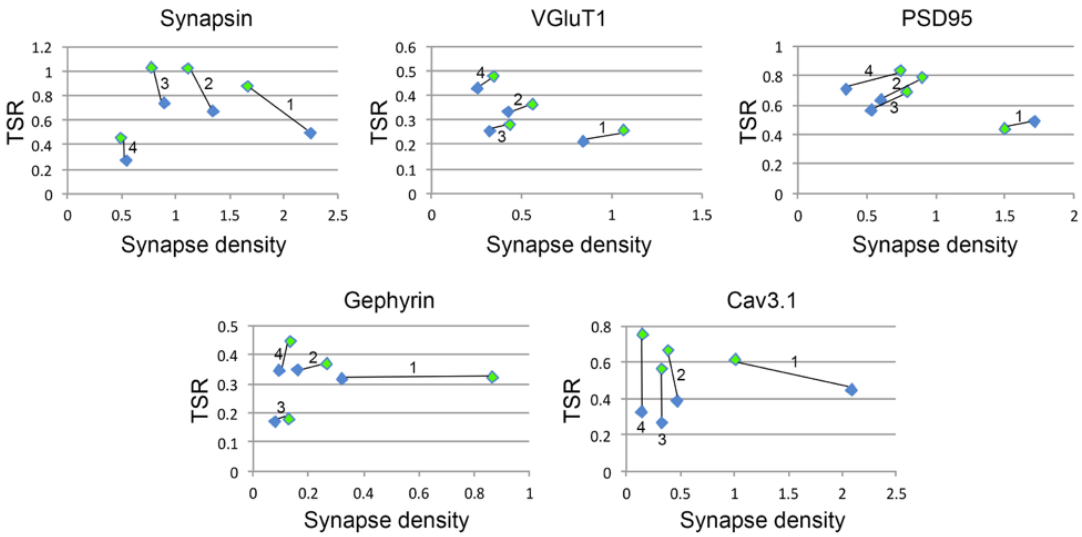

Figure 6. Impact of punctum size requirements on antibody comparisons. Green dots represent the higher scoring antibody, blue dots show the lower scoring one. Each scatter plot shows the results of the comparison of two antibodies against the same target protein while varying the minimum synapse size requirements (numbered 1 through 4). Query 1: one slice of tested antibody, 1 slice control. Query 2: two slices of tested antibody, 1 slice control. Query 3: two slices of tested antibody, 2 slices control. Query 4: three slices of tested antibody, 1 slice control. Query 3 is the original query with its results presented in Table 1. All queries gave consistent results for all five antibody pairs, with the exception of Query 1.

The above results were based on a query requiring both the tested antibody and the control antibody to be present on a minimum of two slices (as expected from the data resolution). To evaluate the robustness of our method, the same comparisons were performed using queries with smaller (only one slice) and larger (three slices) minimum synapse size requirements. For each pair of antibodies, the synapse density and target specificity ratio were computed for each of four combinations (see legend to Figure 6 for details). All queries gave consistent results for all five antibody pairs, except for Query 1, which defined a synapse as spanning only one slice; in two out of the five cases, Query 1 failed to unequivocally identify the otherwise highest scoring antibody. Thus, the use of even limited three-dimensional information from immunolabeling on serial sections as in Queries 2-4, enabled robust quantification of antibody performance.

This experiment illustrates the power and breadth of the proposed method. The queries can

be designed by the user to take into account resolution, synapse type, and antibody binding target. Multiple queries can be run, and the antibody performance can be objectively evaluated with multiple measurements.

Concentration Comparisons

The optimal concentration of an antibody, which reflects both the binding affinity for its target protein in that application and the abundance of the target protein in the particular sample, must be determined experimentally. Use of an excessive concentration of the antibody will lead to high background labeling (false positives), while a suboptimal concentration will lead to sparse labeling (false negatives), due to a failure to label all of the available specific binding sites. Our characterization method was used to quantify the effects of antibody concentration on immunolabeling of AT sections, as evaluated by the synapse density and target specificity ratio measures. The expectation is that as the antibody concentration decreases, the synapse density will decrease, while the target specificity ratio may increase.

Target Protein	Tested antibodies	Control Antibody	Punctum Density/ μm^3	Average Punctum Size / standard deviation (pixels)	Synapse Density/ μm^3	Target Specificity Ratio
Synapsin	SynCS 1:100	VGluT1	1.23	41.6 / 133.6	0.83	0.68
	SynCS 1:1000		1.31	35.9 / 95.9	0.82	0.62
GluA1	GluR1 1:25	VGluT1	0.62	7.9 / 51.8	0.12	0.19
	GluR1 1:125		0.43	9.5 / 41.4	0.08	0.18
	GluR1 1:625		0.18	19.3 / 180.9	0.05	0.27
	GluR1 1:3125		0.13	38.7 / 111.7	0.03	0.21
GluA2	GluR2 1:25	Synapsin	0.89	10.6 / 62.3	0.45	0.5
	GluR2 1:125		0.46	13.9 / 29.5	0.3	0.66
	GluR2 1:625		0.27	17.7 / 82.1	0.18	0.67
	GluR2 1:3125		0.23	15.9 / 103.8	0.13	0.57
GluA3	GluR3 1:25	VGluT1	1.99	6.5 / 11.8	0.42	0.21
	GluR3 1:125		0.81	8.4 / 10.4	0.23	0.28
	GluR3 1:625		0.26	10.8 / 23.5	0.07	0.27
	GluR3 1:3125		0.17	20.6 / 154.1	0.05	0.26
GluN1	NR1 1:25	VGluT1	1	37.2 / 1541.0	0.72	0.72
	NR1 1:125		0.88	17.8 / 208.2	0.63	0.72
	NR1 1:625		0.58	22.0 / 748.9	0.37	0.64
	NR1 1:3125		0.64	9.8 / 54.5	0.39	0.62

Table 2. Five antibodies were evaluated at different concentrations. In all experiments, a control presynaptic antibody was included at its optimal concentration. The detected synapse density decreases as the antibody concentration decreases.

Datasets generated from a series of dilutions were prepared, as shown in Table 2 and Figure 7. For each dataset except GluN1, the minimum expected marker size (query) was the same, a minimum punctum size of 0.2x0.2x0.14μm, corresponding to 2 pixels by 2 pixels by 2 slices. The minimum

punctum size for GluN1 spanned only one slice (0.2x0.2x0.07 μm) because inaccuracies in the alignment of this dataset caused inconsistencies in the positions of synapses on adjacent slices. First, we tested the effect of a 10-fold change in concentration of an antibody against the general presynaptic marker synapsin, imaged in conjunction with immunolabeling for another presynaptic marker, VGluT1. The remaining datasets tested four sequential 5-fold concentration changes on immunolabeling with different glutamate receptor antibodies, as evaluated against immunolabeling with antibodies against a general presynaptic marker (synapsin) or a marker of glutamatergic synapses (VGluT1). Synapsin, previously identified as a particularly robust synaptic antibody for AT, performed equally well over the 10-fold concentration range as evaluated by both the synapse density and target specificity ratio measurements. For each of the glutamate receptor antibodies, the measured synapse density value decreased with increasing dilutions, as expected, while the target specificity value showed no consistent changes. In practical terms, we estimated that the optimal working range of the glutamate receptor antibodies is within a dilution range of 1:25 to 1:125; further dilutions led to missing too many synapses without a substantial improvement in target specificity.

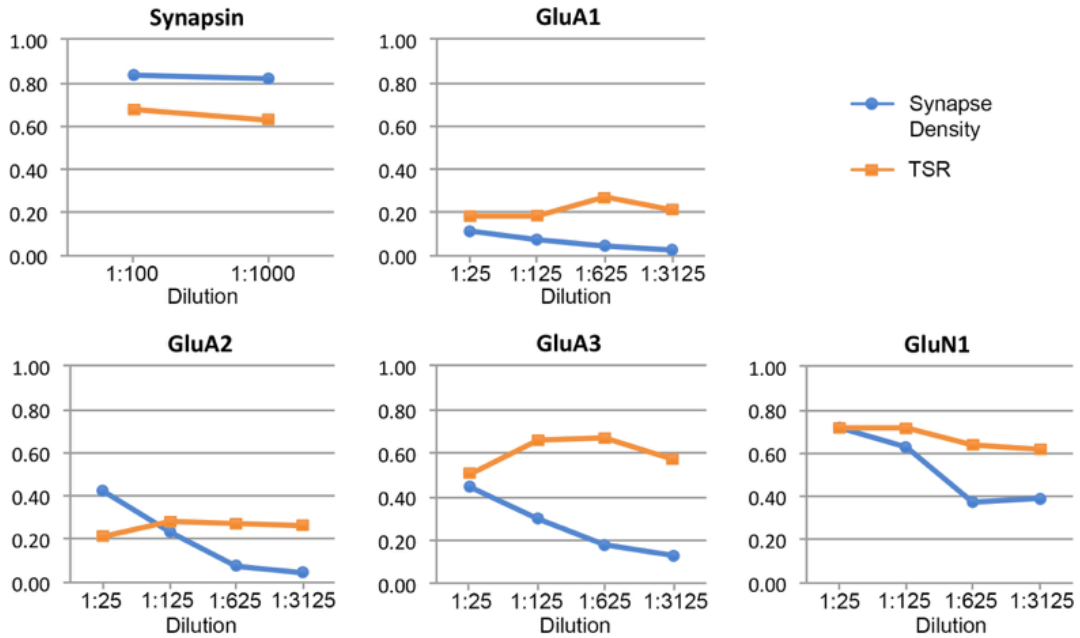

Figure 7. Changes in synapse density and target specificity ratio (TSR) as a function of antibody concentration. Each plot shows the synapse density and target specificity ratio at different concentrations of the same antibody.

Automated Ranking of Candidate Monoclonal Antibodies

The generation of monoclonal antibodies begins with a high-throughput screening procedure that leads to identification of numerous candidate antibodies from each project, which must then be further evaluated. Because only a small fraction of these candidate antibodies will likely exhibit robust and specific immunoreactivity in any given application or sample preparation condition (***Gong et al., 2016***), it is advantageous to screen as many candidate antibodies as possible, for each application. While some common antibody screens have been effectively automated (e.g., ELISA screens), screening on plastic sections from mammalian brain for antibodies that immunolabel specific populations of synapses must still be performed and analyzed manually by an expert observer, a difficult and labor-intensive process. The methods we outline here could be extremely valuable for performing this type of large-scale screen on tissue sections. Accordingly, we tested the performance of our method in screening candidate monoclonal antibodies against synaptic

target proteins generated at the UC Davis/NIH NeuroMab facility. Unfortunately, the concentration of antibody in hybridoma tissue culture supernatants is unknown, so immunolabeling must be performed at antibody concentrations that may differ for different candidate antibodies, and these concentrations may not be optimal.

We imaged AT sections immunolabeled with a set of candidate antibodies against the same target protein. For each dataset, tissue from mouse neocortex was prepared using standard AT methods and had at least two antibodies applied - the candidate antibody for the target protein of interest (used as an undiluted tissue culture supernatant of unknown antibody concentration), and a validated antibody at its optimal concentration. The ranking of candidate antibodies was determined based on the computed synapse density and the target specificity ratio derived from our automated synapse detection algorithm. The target specificity ratio was the deciding factor in most cases; synapse density was used to exclude candidate antibodies which gave unreasonably high values based on previous biological knowledge: excitatory synapses are expected to have a density of approximately 1 per μm^3, and the inhibitory synapses approximately 0.15 per μm^3 (***Calverley and Jones, 1987***; ***Schüz and Palm, 1989***). Each dataset was also (blindly) evaluated and ranked by an expert observer, based on visual examination of the images. Screening of bassoon candidate antibodies was performed in two rounds; the second round included only those candidates identified as best or unclear in the first round. The experiments addressed several questions: 1) Can our algorithm be used to correctly rank the performance of multiple candidate antibodies?; 2) What is the minimum number of control antibodies required to accomplish this?; and 3) What is the optimal query for this type of challenge? Six datasets, ranging from 4 to 19 different candidate antibodies each, were analyzed.

Can our algorithm correctly rank the performance of multiple candidate antibodies?

Analysis of the six datasets confirmed that there was excellent correspondence between the algorithm ranking and expert evaluation of candidate antibody performance. In all but one case, the synapse detection algorithm identified all of the expert-chosen antibodies, and it only missed one in the case of gephyrin, because the group of failed candidate antibodies was too small to serve as an adequate comparison. The results are summarized in Table 3 and Figure 8.

Target Protein	Control antibodies	Total # candidate antibodies tested	# good candidates chosen by expert	# good candidates chosen by algorithm	algorithm false negatives	algorithm false positives
Gephyrin	GAD	7	5	4	1	0
Homer	PSD-95	4	1	1	0	0
IRSP53	PSD-95, VGluT1	12	2	2	0	0 (+1 unclear)
VGAT	GAD	17	4	4	0	0 (+2 unclear)
Collybistin	GAD	19	6	6	0	1
Bassoon 1st exp.	Synapsin	19	4	4	0	0 (+1 unclear)
Bassoon 2nd exp.	VGluT1, PSD-95	10	5	5	0	0

Table 3. Summary of candidate antibody comparisons. Multiple candidate antibodies against the target protein were ranked using measurements from the synapse detection algorithm. The candidate antibodies were independently evaluated by visual inspection of the immunofluorescence images. For each target protein, the control antibodies were chosen according to the known characteristics of synapses expressing the target protein.

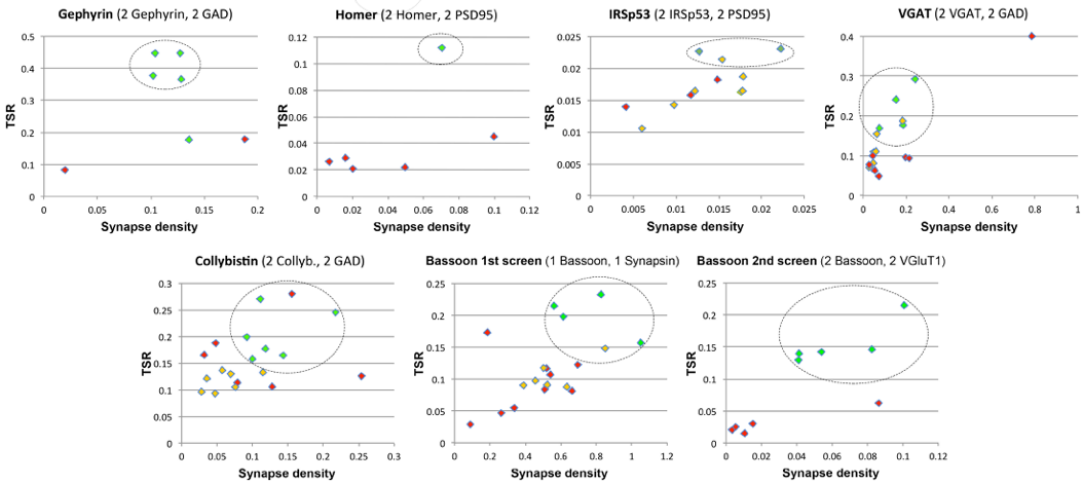

Figure 8. Comparison of multiple candidate antibodies. Each scatter plot shows the computed synapse density and target specificity ratio of multiple candidate antibodies, with the best-ranking candidates circled. Expert ranking is color-coded: green - best, orange - unclear, red - fail. The specific query in each case is indicated in the plot title, where the number indicates the minimum punctum size for each label. For example, '2 Gephyrin, 2 GAD' means that a synapse in this case is defined as a gephyrin punctum that spans at least 2 slices adjacent to a GAD punctum that also spans at least 2 slices. The outlier in the VGAT scatter plot was not included in the best candidate antibodies selection, because of the abnormally high synaptic density (0.7 per μm^3 compared to target max density of 0.15 per μm^3). Screening of the bassoon project was performed in 2 rounds: the candidate antibodies identified as best or unclear in the first round were screened again with adjusted concentrations.

What is the minimum number of control antibodies?

The previous experiments with pairwise or concentration comparisons were performed using only one control antibody. In those cases, the tested antibodies were already known to recognize

their target in plastic sections and it was therefore reasonable to assume that the combination of one control synaptic antibody with one tested synaptic antibody will generate synapse-specific data. However, this is not the case when screening multiple candidate antibodies with unknown performance in the AT application. To verify whether in the present case an additional control antibody may offer an advantage, two of the datasets included both presynaptic and postsynaptic control antibodies. In these two datasets, the performance of the query containing an additional control antibody was compared to the standard single control antibody query used in the previous experiments. In both cases, the results of the two queries were very similar (compare Figure 9 with Figure 8), suggesting that the inclusion of a second control synaptic antibody is unnecessary for the purpose of screening large sets of candidate antibodies.

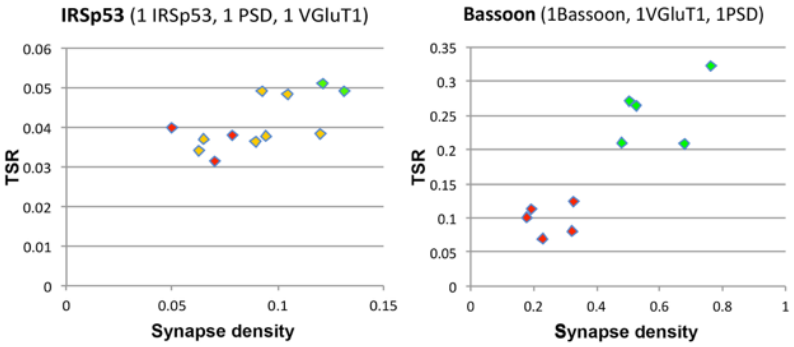

Figure 9. Comparison of multiple candidate antibodies using two control synaptic antibodies. The specific query in each case is indicated in the plot title. For example IRSp53, PSD, VGluT1 means that a synapse is defined as the colocalization of an IRSp53, PSD-95 and VGluT1 punctum. Expert ranking is color coded: green - best, orange - unclear, red - fail. Compare with Figure 8.

What is the optimal query?

The pairwise antibody comparison experiments showed that the results were not affected by the stringency of the query, except in cases when the query was too permissive (smallest synapse size: labels present on 1 slice). Therefore, to screen multiple candidate antibodies, we generally chose queries of medium stringency, requiring the labels to be present in two consecutive slices. This strategy worked very well for candidate antibodies directed against abundant synaptic proteins (gephyrin, homer1, IRSp53, VGAT, collybistin). In contrast, the permissive query, which required the labels to be present on only one section, gave inconclusive results in most of these cases (Figure 10). The first round of screening for bassoon antibodies was an exception, because it yielded clearer results with a one-section query. This is likely due to the wide variations in concentration of the candidate antibodies present in the tissue culture supernatants used for screening, many of which required subsequent dilution, as performed in the second round of testing. In this second round with adjusted concentrations, the two-section query performed well, as seen for the other abundant synaptic target proteins. These experiments suggest that it is best to start an antibody evaluation using a query that requires the labels to be present in two slices. The top-ranking antibodies based on such a query are then selected and visually examined by experts to confirm their performance.

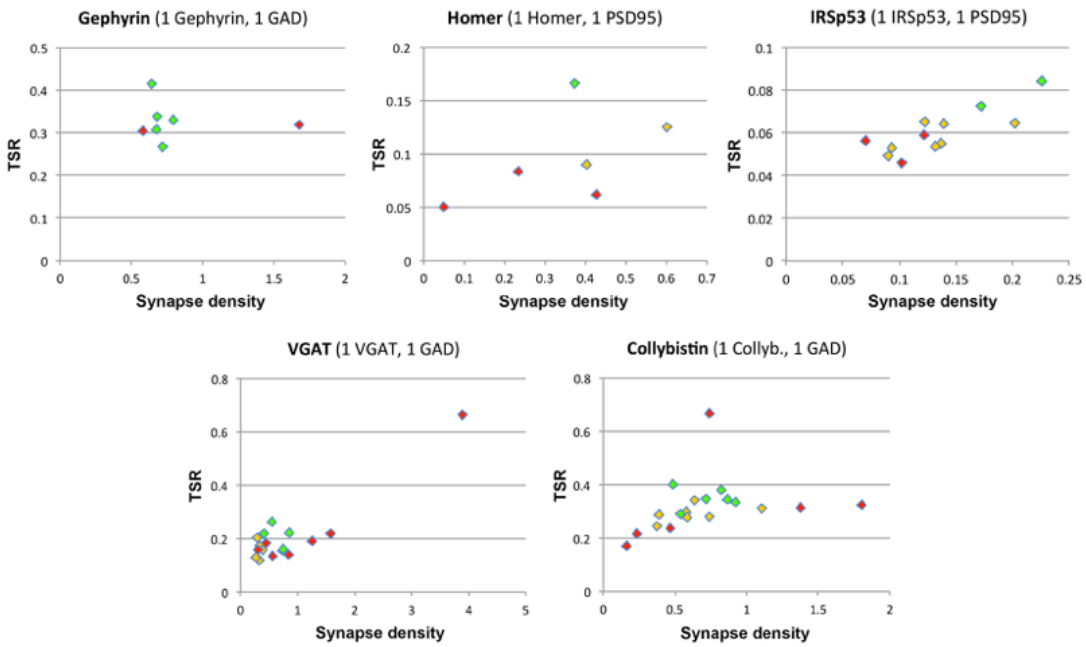

Figure 10. Comparison of multiple candidate antibodies and queries. These plots compare multiple candidate antibodies using an alternative query requiring the puncta to be present on only 1 slice, instead of 2 as in Figure 8. Each scatter plot shows the synapse density and target specificity ratio of multiple candidate antibodies against the same target protein. Expert ranking is color coded: green - best, orange - unclear, red - fail. The specific query in each case is indicated in the plot title, where the number indicates the minimum punctum size for each label. In many of these cases (gephyrin, VGAT, collybistin), the more permissive 1-slice query does not allow correct selection of the best performing candidate antibodies.

Discussion

The present work introduces a highly effective approach for automated characterization and screening of antibodies for AT. Our approach uses the probabilistic synapse detection algorithm described in ***Simhal et al.*** (***2017***), which is expanded here to provide a quantitative and objective assessment of antibody performance. The output of this algorithm is a number of automatically computed characteristics such as synapse density and target specificity ratio, that reflect the sensitivity and specificity of immunolabeling with a given antibody. These are just examples of characteristics that can be easily computed with the automatic synapse detection algorithm. Taken together, these computed characteristics provide an objective way to characterize and compare the performance of different antibodies against the same target, simplifying the process for selecting antibodies best suited for AT. When evaluating multiple candidate antibodies, this represents an efficient method to identify a small number of promising antibodies for further evaluation.

The probabilistic synapse detector was designed to provide a flexible tool for antibody screening. Because it is query-based, it allows the user to define the molecular composition and size of synapses expected to contain the antigen. This flexibility is advantageous for synaptic antibody screening because the query can be designed to focus on different synapse subtypes, depending on prior biological knowledge (e.g., what combinations of proteins are likely to be present, and where the antibody target is expected to be located). Its inherent flexibility should allow this approach to be used also to validate antibodies that target other subcellular structures, ranging from the nodes of Ranvier on myelinated axons, to mitochondria, to histone marks in the nucleus. The method works with a wide selection of control antibodies, which need not colocalize with the tested antibody. For example, antibodies to gephyrin and collybistin, both postsynaptic proteins, were evaluated using the presynaptic marker GAD as control. The flexibility in control antibody selection

enables researchers to optimize the use of their available antibody stocks. With further practical experience we anticipate that a restricted group of well-characterized antibodies will be adopted as controls for each target category.

Our experiments demonstrate that the probabilistic synapse detector is a robust tool for antibody screening, allowing the objective ranking of antibodies based on quantitative measures of their performance. In the pairwise comparisons of antibodies, there was 100% agreement between the expert ranking and the automated antibody ranking based on synapse density and target selectivity ratio. Variations in the query did not affect the ranking, as long as synapse detection was based on more than one slice. Even when a synapse was required to be present on only one slice, performance was only modestly degraded, such that the outcome measures for some antibody pairs were ambiguous. The present approach also accommodates variations in antibody concentration, as demonstrated by the experiments with multiple candidate antibodies from monoclonal antibody projects, which showed a very high correlation between the ranking by algorithm and by expert evaluation of candidate antibody performance in all six datasets, even though the concentration of antibodies in the hybridoma tissue culture supernatants used for screening was unknown and intrinsically variable. This insensitivity to antibody concentration is very important in practice when evaluating multiple antibodies, because it significantly reduces the amount of work involved by eliminating the need of immunolabeling with series of antibody dilutions.

There are some limitations to the use of the probabilistic synapse detector as an antibody characterization tool. This is not a stand-alone tool for antibody validation; it is designed to specifically address the performance of the antibody for immunofluorescence AT on plastic sections, and must be used along with other tests and controls. For example, the method does not test for cross-reactivity with other proteins. A second limitation is that this approach requires prior knowledge of the expected distribution of the antigen, especially if it is found only in a small population of synapses. In such cases it will be important to ensure that the tissue sample used for immunolabeling contains such synapses at a reasonable density and/or includes a control marker to independently identify this population. A number of technical issues can interfere with performance. The probabilistic synapse detector performs best with queries that require a synapse to be present on at least two consecutive sections; accordingly, proper alignment of the sections in the imaged series is required to ensure that position of synapses is consistent on adjacent sections. In one of the concentration comparison experiments with GluN1, inaccuracies in the alignment led to poor performance of the algorithm when using the standard query requiring a synapse to be present on at least two consecutive sections. In this case, a one-slice query was successfully used, but this approach will not always work, because this query did not perform well on all of the tested datasets. To fully benefit from the advantages of using three-dimensional information from multiple serial slices, one has to ensure that the datasets are well aligned. Another technical issue to consider is possible bleed-through during the fluorescent imaging, which can cause the false impression of colocalization between the tested and control antibodies.

When carefully planned and executed to avoid pitfalls, the automated approach described here can be used to identify and characterize antibodies against a wide assortment of synaptic target proteins that yield robust and specific immunolabeling in plastic sections of brain tissue. This is particularly important because despite extensive work, the nature of synaptic processing is still poorly understood, and many basic questions remain. For example, how many different types of synapse exist? How do these different types vary over different brain areas? How does their distribution change over time? With experience? Under pathological conditions? For questions of this nature, it is important to objectively assess a large number of individual synapses, and a large number of different molecules at each synapse, as can be done using AT. Identifying reliable synaptic antibodies for AT will remove a major limitation for such studies and allow a better understanding

of synapses.

Methods

Data Background

The datasets presented were created from adult mouse neocortical tissue that was prepared, immunolabeled, and imaged using standard methods of AT (***Micheva et al., 2010***; ***Collman et al., 2015***). Briefly, the tissue was chemically fixed using 4% paraformaldehyde in PBS, embedded in LR-White resin and cut into serial ultrathin sections (70 nm), which were mounted onto coverslips. One of the datasets from the automated ranking of the candidate monoclonal antibodies experiments (IRSp53) used tissue prepared in a different way: chemical fixation with 2% paraformaldehyde and 2% gluaraldehyde in PBS, followed by freeze-substitution and embedding in Lowicryl HM20 (***Collman et al., 2015***). The sections were labeled using indirect immunofluorescence and imaged on an automated wide-field fluorescence microscope (Zeiss AxioImager Z1, Zeiss, Oberkochen, Germany) with a 63x Plan-Apochromat 1.4 NA oil objective. While the exact size of the datasets varies, their general structure is consistent.

Antibodies

The antibodies used for the experiments presented here are listed in Table 4. Some of the antibodies used were tested in conjunction with screening of monoclonal antibody projects at the UC Davis/NIH NeuroMab Facility, consistent with our goal to facilitate testing of large panels of candidate antibodies in an efficient and objective fashion.

Target protein	***Host***	***Antibody Source***	***RRID****
Bassoon	Mouse	NeuroMab L124 project	RRID:AB_2716712
Cav3.1	Mouse	NeuroMab 75206	RRID:AB_2069421
Cav3.1	Rabbit	Synaptic Systems 152 503	RRID:AB_2619850
Collybistin	Mouse	NeuroMab L120 project	RRID:AB_ 2650452
GAD2	Rabbit	Cell Signaling 5843	RRID:AB_10835855
Gephyrin BD	Mouse	BD Biosciences 612632	RRID:AB_399669
Gephyrin	Mouse	NeuroMab L106 project	RRID:AB_ 2617120 RRID:AB_ 2617121 RRID:AB_ 2632414
GluA1	Rabbit	Millipore AB1504	RRID:AB_2113602
GluA2	Mouse	Millipore MAB397	RRID:AB_2113875
GluA3	Rabbit	Abcam ab40845	RRID:AB_776310
Homer	Mouse	NeuroMab L113 project	RRID:AB_ 2629418
IRSp53	Mouse	NeuroMab L117 project	RRID:AB_2619741
GluN1	Mouse	Millipore MAB363	RRID:AB_94946
PSD95	Mouse	NeuroMab 75-028	RRID:AB_2292909
PSD95	Rabbit	Cell Signaling 3450	RRID:AB_2292883
Synapsin	Guinea pig	Synaptic Systems 106 004	RRID:AB_1106784
Synapsin	Rabbit	Cell Signaling 5297	RRID:AB_2616578
VGAT	Mouse	NeuroMab L118 project	RRID:AB_2650550
VGluT1	Guinea pig	Millipore AB5905	RRID:AB_2301751
VGluT1	Mouse	NeuroMab 75-066	RRID:AB_2187693

Table 4. Antibodies used in this study. *RRID: Research Resource Identifier. For the NeuroMab projects, the RRID of the finally selected antibodies is listed; this selection was based on multiple factors in addition to the antibody performance evaluated using the current method.

Computational Method

In order to evaluate and automatically characterize antibodies, we computed a series of quantitative measurements by extending the probabilistic query-based synapse detector described in (***Simhal et al., 2017***), which can be expanded depending on specific antibody characterization and screening needs. The measurements selected provide unbiased quantitative information to help evaluate the intensity, specificity and sensitivity of immunolabeling obtained with a given antibody. As the output of our analyses we calculate the *density of puncta*, the *average punctum volume and standard deviation* for each antibody, as well as the *synapse density* (number of detected synapses per volume), and *target specificity ratio* (the ratio of detected synapses to detected candidate antibody puncta); these measures provide the user an immediately useful quantitative assessment of the data.

Detected Density of Puncta

The density of the detected 3D puncta reflects the biological properties of the tissue (i.e., the abundance and distribution of the target protein), as well as the intensity and specificity of the immunolabeling with a given antibody at the concentration used. To determine the number of puncta detected in each channel, probability maps, where the value at every voxel is the probability it belongs to a 3D punctum, are computed and then thresholded. The process is outlined in Figure 11. The 3D punctum density is then calculated as:

$$\text{3D Punctum Density} = \frac{\text{Number of Detected 3D Puncta}}{\text{Total Volume}}$$

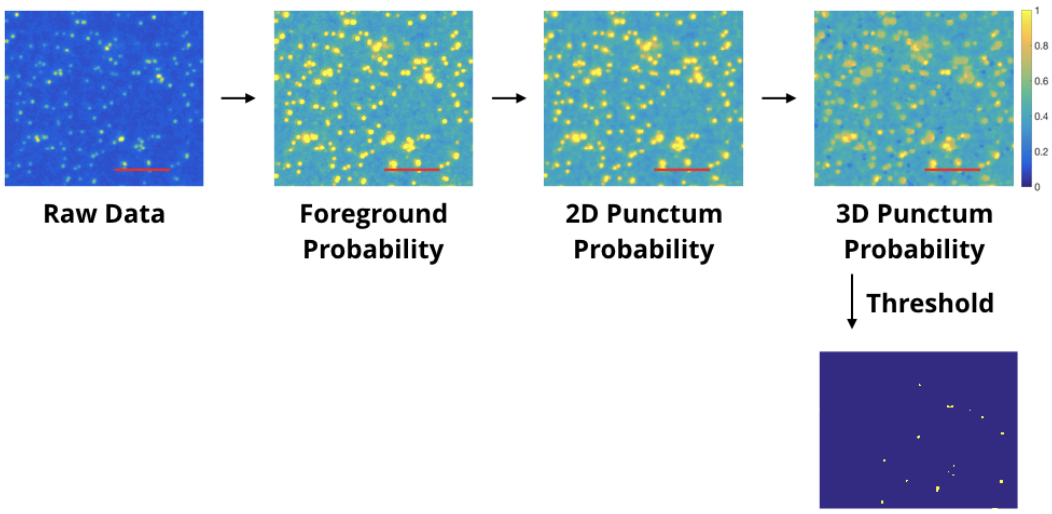

Figure 11. Automated Punctum Detection Pipeline. The first box shows the raw image data from immunolabeling with one antibody. The second box is the output of a 'foreground probability' step; the intensity value of each pixel codes the probability it belongs to the foreground. The third box is the output of a '2D Punctum Probability' step; each pixel codes the probability that it belongs to a 2D blob. The '3D punctum probability' image's intensity values are the probability that a voxel belongs to a blob which spans the minimum number of slices. The thresholded image is shown below. Red scale bars represent 5 μm.

Average Punctum Volume

After segmenting the immunolabeling data, the average volume of each punctum, and the standard deviation in punctum volume are calculated. If the average punctum size is smaller or larger than expected, it may indicate a lack of efficacy and/or specificity for immunolabeling with that antibody. If the standard deviation of punctum volume is large, it may indicate erratic labeling. Figure 12 shows an example displaying a very large standard deviation; a standard deviation this large makes

it unlikely that the candidate antibody on the left will serve as a satisfactory marker for inhibitory (collybistin-positive) synapses. More robust measurements could be considered, such as percentile, if so desired.

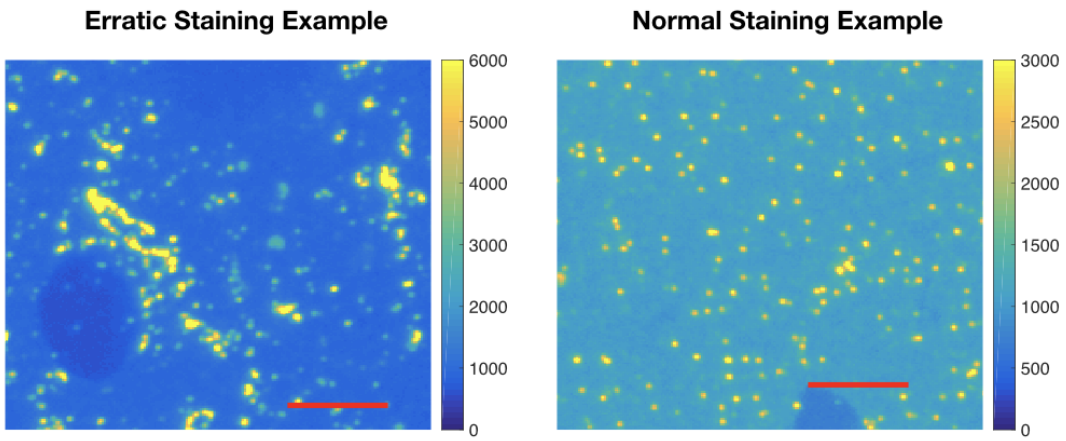

Figure 12. Puncta Labeling Example. (Left) Immunolabeling for collybistin (associated with GABAergic synapses) on a raw IF slice; note the very broad distribution of sizes for puncta. (Right) Relatively 'normal' pattern of immunolabeling on a raw IF slice, using a different collybistin candidate antibody. This difference is automatically quantified by the automated synapse detection framework. Each red scale bar is 5 μm.

Synapse Density

Each dataset has a target protein of interest for which multiple candidate antibodies are tested, alongside a previously-validated synaptic antibody that recognizes a target protein that either lies adjacent to or colocalizes with the target protein of interest. The synapse density of a given volume is computed as

$$\text{Synapse Density} = \frac{\text{Number of Detected Synapses}}{\text{Total Volume}}$$

This measure is useful for evaluating antibodies against targets with a known distribution at synapses, where the density of synapses containing the target protein can be estimated. For example, ubiquitous markers of inhibitory synapses like gephyrin are expected to be present at the large majority of inhibitory synapses, and therefore have a synaptic density in rodent neocortex on the order of 0.15 synapses per μm^3 (***Knott et al., 2002***). A computed synapse density substantially lower than expected may indicate low sensitivity of the antibody and/or insufficient concentration, while a synapse density considerably above that expected likely reflects nonspecific (off-target) binding of the antibody.

Target Specificity Ratio

Target specificity ratio (TSR) represents the fraction of puncta immunolabeled with the candidate antibody that are actually associated with a bona fide synapse, and is computed as

$$\text{TSR} = \frac{\text{Number of Detected Synapses}}{\text{Number of Detected 3D Puncta}}$$

The higher the TSR, the lower is the magnitude of the nonsynaptic labeling obtained with that candidate antibody. Interpretation of this measurement will depend on the specific target; some proteins associated with synapses are almost exclusively present at synapses (e.g., synapsin), while others are also found at locations outside of the synapse (e.g., glutamate receptors). Therefore, the target specificity reflects both the biological distribution of the target protein, and any non-specific

binding of the candidate antibody. When comparing two antibodies against the same antigen, differences in target specificity reflect differences in their specificity.

Acknowledgments

This work was supported by the National Institutes of Health (NIH-TRA 1R01NS092474, R01NS094499, R01MH111768, R24 NS092991, and R01NS039444.) and the Allen Institute for Brain Sciences (AIBS), along with the National Science Foundation (NSF), United States Office of Naval Research (ONR), United States Army Research Office (ARO), and the National Geospatial Intelligence Agency (NGA).

References

Anderson CN, Grant SG. High throughput protein expression screening in the nervous system–needs and limitations. The Journal of physiology. 2006; 575(2):367–372.

Andersson S, Sundberg M, Pristovsek N, Ibrahim A, Jonsson P, Katona B, Clausson CM, Zieba A, Ramström M, Söderberg O, et al. Insufficient antibody validation challenges oestrogen receptor beta research. Nature Communications. 2017; 8:ncomms15840.

Ayala R, Kett LR, Leach TL, Young AB, Dunah AW, Orlando LR. Metabotropic glutamate receptor 1 (mGluR1): antibody specificity and receptor expression in cultured primary neurons. Journal of neuroscience methods. 2012; 204(2):221–226.

Baker M. Blame it on the antibodies. Nature. 2015; 521(7552):274.

Bass C, Helkkula P, De Paola V, Clopath C, Bharath AA. Detection of axonal synapses in 3D two-photon images. PloS one. 2017; 12(9):e0183309.

Bordeaux J, Welsh AW, Agarwal S, Killiam E, Baquero MT, Hanna JA, Anagnostou VK, Rimm DL. Antibody validation. Biotechniques. 2010; 48(3):197.

Burette A, Collman F, Micheva KD, Smith SJ, Weinberg RJ. Knowing a synapse when you see one. Frontiers in neuroanatomy. 2015; 9.

Busse B, Smith S. Automated analysis of a diverse synapse population. PLoS computational biology. 2013; 9(3):e1002976.

Calverley R, Jones D. A serial-section study of perforated synapses in rat neocortex. Cell and tissue research. 1987; 247(3):565–572.

Collman F, Buchanan J, Phend KD, Micheva KD, Weinberg RJ, Smith SJ. Mapping synapses by conjugate light-electron array tomography. Journal of Neuroscience. 2015; 35(14):5792–5807.

Fantuzzo J, Mirabella V, Hamod A, Hart R, Zahn J, Pang Z. Intellicount: High-Throughput Quantification of Fluorescent Synaptic Protein Puncta by Machine Learning. eNeuro. 2017; 4(6):ENEURO–0219.

Fritschy JM, Weinmann O, Wenzel A, Benke D. Synapse-specific localization of NMDA and GABAA receptor subunits revealed by antigen-retrieval immunohistochemistry. Journal of Comparative Neurology. 1998; 390(2):194–210.

Fukaya M, Watanabe M. Improved immunohistochemical detection of postsynaptically located PSD-95/SAP90 protein family by protease section pretreatment: A study in the adult mouse brain. Journal of Comparative Neurology. 2000; 426(4):572–586.

Gong B, Murray KD, Trimmer JS. Developing high-quality mouse monoclonal antibodies for neuroscience research–approaches, perspectives and opportunities. New biotechnology. 2016; 33(5):551–564.

Gong B, Rhodes KJ, Bekele-Arcuri Z, Trimmer JS. Type I and type II Na+ channel α-subunit polypeptides exhibit distinct spatial and temporal patterning, and association with auxiliary subunits in rat brain. Journal of Comparative Neurology. 1999; 412(2):342–352.

Griffiths G, Lucocq JM. Antibodies for immunolabeling by light and electron microscopy: not for the faint hearted. Histochemistry and cell biology. 2014; 142(4):347–360.

Knott GW, Quairiaux C, Genoud C, Welker E. Formation of dendritic spines with GABAergic synapses induced by whisker stimulation in adult mice. Neuron. 2002; 34(2):265–273.

Kreshuk A, Koethe U, Pax E, Bock DD, Hamprecht FA. Automated detection of synapses in serial section transmission electron microscopy image stacks. PloS one. 2014; 9(2):e87351.

Lorincz A, Nusser Z. Specificity of immunoreactions: the importance of testing specificity in each method. Journal of Neuroscience. 2008; 28(37):9083–9086.

Manning CF, Bundros AM, Trimmer JS. Benefits and pitfalls of secondary antibodies: why choosing the right secondary is of primary importance. PloS one. 2012; 7(6):e38313.

Micheva KD, Busse B, Weiler NC, O'Rourke N, Smith SJ. Single-synapse analysis of a diverse synapse population: proteomic imaging methods and markers. Neuron. 2010; 68(4):639–653.

Micheva KD, Smith SJ. Array tomography: a new tool for imaging the molecular architecture and ultrastructure of neural circuits. Neuron. 2007; 55(1):25–36.

Nilsson P, Paavilainen L, Larsson K, Ödling J, Sundberg M, Andersson AC, Kampf C, Persson A, Szigyarto CAK, Ottosson J, et al. Towards a human proteome atlas: High-throughput generation of mono-specific antibodies for tissue profiling. Proteomics. 2005; 5(17):4327–4337.

O'rourke NA, Weiler NC, Micheva KD, Smith SJ. Deep molecular diversity of mammalian synapses: why it matters and how to measure it. Nature Reviews Neuroscience. 2012; 13(6):365–379.

Rhodes KJ, Trimmer JS. Antibodies as valuable neuroscience research tools versus reagents of mass distraction. Journal of Neuroscience. 2006; 26(31):8017–8020.

Saper CB. An open letter to our readers on the use of antibodies. Journal of Comparative Neurology. 2005; 493(4):477–478.

Saper CB. A guide to the perplexed on the specificity of antibodies. Journal of Histochemistry & Cytochemistry. 2009; 57(1):1–5.

Schüz A, Palm G. Density of neurons and synapses in the cerebral cortex of the mouse. Journal of Comparative Neurology. 1989; 286(4):442–455.

Sheng M, Kim E. The postsynaptic organization of synapses. Cold Spring Harbor perspectives in biology. 2011; 3(12):a005678.

Simhal AK, Aguerrebere C, Collman F, Vogelstein JT, Micheva KD, Weinberg RJ, Smith SJ, Sapiro G. Probabilistic fluorescence-based synapse detection. PLoS computational biology. 2017; 13(4):e1005493.

Uhlen M, Bandrowski A, Carr S, Edwards A, Ellenberg J, Lundberg E, Rimm DL, Rodriguez H, Hiltke T, Snyder M, et al. A proposal for validation of antibodies. Nature methods. 2016; .

Weiler NC, Collman F, Vogelstein JT, Burns R, Smith SJ. Synaptic molecular imaging in spared and deprived columns of mouse barrel cortex with array tomography. Scientific data. 2014; 1:140046.

Wilhelm BG, Mandad S, Truckenbrodt S, Kröhnert K, Schäfer C, Rammner B, Koo SJ, Claßen GA, Krauss M, Haucke V, et al. Composition of isolated synaptic boutons reveals the amounts of vesicle trafficking proteins. Science. 2014; 344(6187):1023–1028.